

Vibrational spectroscopy of hydrated electron clusters $(\text{H}_2\text{O})_n^-$ via infrared multiple photon dissociation

Knut R. Asmis^{a),b)}*Fritz-Haber-Institut der Max-Planck-Gesellschaft, Faradayweg 4-6, D-14195 Berlin, Germany*

Gabriele Santambrogio

Institut für Experimentalphysik, Freie Universität Berlin, Arnimallee 14, D-14195 Berlin, Germany

Jia Zhou and Etienne Garand

Department of Chemistry, University of California, Berkeley, California 94720

Jeffrey Headrick

Sterling Chemistry Laboratory, Yale University, P.O. Box 208107, New Haven, Connecticut 06520

Daniel Goebbert

*Fritz-Haber-Institut der Max-Planck-Gesellschaft, Faradayweg 4-6, D-14195 Berlin, Germany*Mark A. Johnson^{a),c)}*Sterling Chemistry Laboratory, Yale University, P.O. Box 208107, New Haven, Connecticut 06520*Daniel M. Neumark^{a),d)}*Department of Chemistry, University of California, Berkeley, California 94720**and Chemical Sciences Division, Lawrence Berkeley National Laboratory, Berkeley, California 94720*

(Received 30 March 2007; accepted 26 April 2007; published online 21 May 2007)

Infrared multiple photon dissociation spectra for size-selected water cluster anions $(\text{H}_2\text{O})_n^-$, $n = 15-50$, are presented covering the frequency range of $560-1820\text{ cm}^{-1}$. The cluster ions are trapped and cooled by collisions with ambient He gas at 20 K, with the goal of defining the cluster temperature better than in previous investigations of these species. Signal is seen in two frequency regions centered around 700 and $1500-1650\text{ cm}^{-1}$, corresponding to water librational and bending motions, respectively. The bending feature associated with a double-acceptor water molecule binding to the excess electron is clearly seen up to $n=35$, but above $n=25$; this feature begins to blueshift and broadens, suggesting a more delocalized electron binding motif for the larger clusters in which the excess electron interacts with multiple water molecules. © 2007 American Institute of Physics. [DOI: 10.1063/1.2741508]

Hydrated electrons play an important role in radiation chemistry, particularly as intermediates in the primary events leading to irreversible damage in cells. A molecular level understanding of electron solvation, knowledge of which is fundamental to the understanding of basic solute-solvent phenomena, has emerged as one of the outstanding problems in contemporary chemical physics. Structural information on the hydrated electron was initially obtained by electron spin resonance of electrons in 10M sodium hydroxide aqueous glass,¹ which indicated that the electron is surrounded by six water molecules, each singly hydrogen bound to the electron, in an octahedral configuration. Interestingly, the electron spin-echo patterns were later reinterpreted² and attributed to just two protons in the first solvation shell. In spite of this correction, the original octahedral model persists, and molecular dynamics simulations³ with this configuration indeed captured most aspects of transient absorption spectra of solvated electrons.⁴ Recent resonance Raman studies on aque-

ous solvated electrons^{5,6} showed strongly enhanced, moderately redshifted intramolecular bending and blueshifted libration modes compared to bulk water and were also interpreted within the context of the original octahedral model. In this paper, we investigate electron hydration from a different perspective, namely, the vibrational spectroscopy of water cluster anions $(\text{H}_2\text{O})_n^-$.

Finite water cluster anions⁷ have drawn considerable attention, as they represent potential model systems for characterizing the water network accommodating the excess electron under well-controlled conditions and as a function of size. Structural information from experiments and calculations on isolated hydrated electron clusters has, however, remained controversial, in part owing to the absence of thermal equilibrium of the ion population in cluster beam sources, resulting in the production of metastable species. Photoelectron spectroscopy of negatively charged water clusters found evidence for (at least) three isomeric classes I-III, characterized by different vertical electron detachment energies (VDEs), which evolve smoothly with cluster size.^{8,9} The relaxation and optical properties of the most stable isomer class (class I) extrapolate to bulk limits and were consequently associated with isomeric structures that evolve to-

^{a)}Authors to whom correspondence should be addressed.

^{b)}Electronic mail: asmis@fhi-berlin.mpg.de

^{c)}Electronic mail: mark.johnson@yale.edu

^{d)}Electronic mail: dneumark@berkeley.edu

ward internally solvated clusters.^{10,11} Quantum simulations by Landman and Jortner¹² anticipated two isomer classes based on the surface versus internal solvation morphology, predicting they could be distinguished by their VDE's, with the internal states yielding higher VDEs. More recent simulations by Turi and Rossky¹³ confirmed two isomer classes, but interpreted the observed electronic absorption spectra¹⁴ and VDE's in terms of surface states. These simulations predicted that interior-bound electrons become energetically favorable only at considerably larger cluster sizes than have been studied thus far.

More detailed insight into the structure and binding in hydrated electron clusters comes from infrared (IR) photodissociation studies.^{15–17} Vibrational action spectra of bare $(\text{H}_2\text{O})_n^-$ clusters were measured in the OH stretching region up to $n=21$, but the $n>9$ spectra suffered from thermal broadening. Vibrational predissociation spectra of bare ($n=15$) and Ar-tagged ($n=3–24$) hydrated electron clusters were also measured in the water bending region, establishing the double H-bond acceptor (AA) motif for small- and medium-sized ($n<24$) type I clusters.¹⁶ The AA motif is characterized by a uniquely redshifted bending band in the 1500–1550 cm^{-1} region, due to significant charge transfer into the O–H σ^* orbitals,¹⁸ and resulting in VDE's comparable to those measured for type I clusters.¹⁹ The more weakly binding type II clusters do not display the AA feature,¹⁷ but instead contribute broad structure at intermediate redshifts. These results raise the interesting question of whether the AA motif is specific to smaller clusters or if it persists in larger clusters and possibly in the bulk phase, as originally hinted at by Dikanov and Tsvetkov.² These studies also suggest that a classification of the isomer classes based on the nature of the local binding site of the hydrated electron, rather than the original concept of internal versus surface hydration, may be more useful, at least for smaller clusters.¹⁷

Here, we study the vibrational spectroscopy of $(\text{H}_2\text{O})_n^-$ clusters from $n=15$ –50 in the water bending and, for the first time, librational regions of the spectrum, directly addressing the question related to the persistence of the AA motif. Moreover, the ions are trapped and “adiabatically” cooled through many collisions with He atoms, substantially reducing the complexity, compared to previous experiments, introduced by the likely presence of kinetically trapped, metastable isomers.⁹

Experiments were carried out on a previously described tandem mass spectrometer-ion trap system²⁰ using radiation from the broadly tunable free electron laser for IR experiments (FELIX).²¹ Water-cluster anions were generated by passing 30 psi (gauge) of Ar over H_2O prior to supersonic expansion into a vacuum through an Even-Lavie pulsed valve²² operating at a 40 Hz repetition rate. The gas pulse was crossed by high-energy electrons (~ 500 eV), generating anions through secondary-electron attachment near the throat of the expansion.²³ The ion beam, comprising a distribution of cluster ions of different sizes, exits the source region, after which it is collimated in space in a gas-filled radio frequency (rf) ion guide and directed into the first quadrupole mass filter. Mass-selected ions are then guided into a temperature-

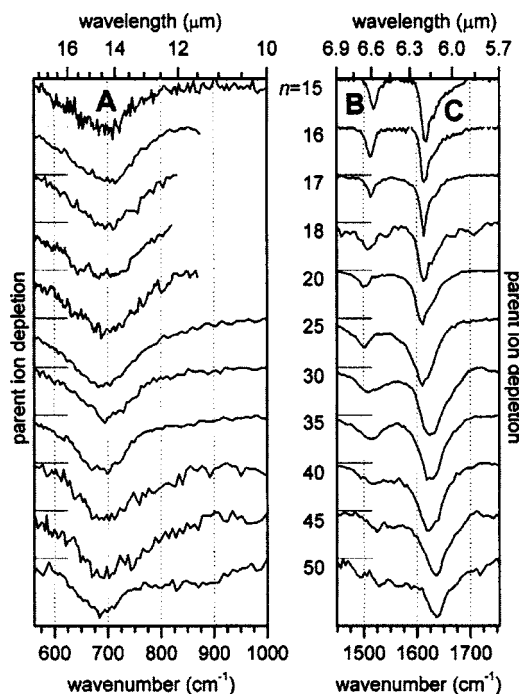


FIG. 1. IRMPD spectra $(\text{H}_2\text{O})_n^-$ clusters ranging from $n=15$ to $n=50$ in the region of the water libration (560–1000 cm^{-1}) and the water bend modes (1450–1755 cm^{-1}). The parent ion yield is plotted as a function of the irradiation wavelength (top axis) and corresponding wave number (bottom axis). Each individual spectrum has been normalized to its strongest depletion feature. The three main depletion features are labeled A, B, and C, respectively.

adjustable linear rf ion trap. For the present experiments the ion trap was held at 20 K. Trapped cluster ions are cooled by collisions with the continuously flowing buffer gas (0.08 mbar). IR multiple photon dissociation (IRMPD) spectra²⁴ are measured in the range from 5.5 to 18 μm (1820–560 cm^{-1}) and at a repetition rate of 5 Hz by photoexcitation of the trapped ions with the pulsed free electron laser radiation and subsequent monitoring of the parent ion signal (depletion measurement). For larger clusters ($n>24$), dissociation of the parent cluster is the dominant depletion mechanism, while for smaller clusters electron detachment also contributes.²⁵

IRMPD spectra of hydrated electron clusters $(\text{H}_2\text{O})_n^-$, obtained for cluster sizes ranging from $n=15$ to 50, are shown in Fig. 1. The spectra have been normalized to the most intense feature in each individual spectrum. In the $n=15$ spectrum, three absorption features, labeled A–C in Fig. 1, are observed: a weak and broad feature at ~ 700 cm^{-1} (A) and two narrower and more intense bands at 1518 (B) and 1618 cm^{-1} (C). The relative intensities of these bands, determined from overview spectra (not shown), change with cluster size, as do their widths. For the smaller clusters, the most prominent feature is band C, followed by band B and then A. Band B loses intensity relative to C and A with increasing cluster size. Band C broadens considerably with increasing cluster size, while band A remains similar in shape and becomes the most prominent feature in the spectra of the larger clusters. The relative areas of bands A and C roughly scale with the number of water molecules, while that of band B clearly does not.

Bands B and C for $(\text{H}_2\text{O})_{15}^-$ in Fig. 1 match those seen previously for bare $(\text{H}_2\text{O})_{15}^-$.¹⁶ Both bands were assigned to water bending modes; the higher frequency band (band C in our spectra) was attributed to water molecules interacting only weakly with the extra electron, while the strongly redshifted band (band B in Fig. 1) was assigned to the unique double H-bond acceptor (AA) water molecule, the binding site of the excess electron. The unstructured band A has not been observed before in the gas phase, but is known from condensed phase spectra and is assigned to water librational modes. It lies close to the corresponding band observed at 685 cm^{-1} in liquid water (at $0\text{ }^\circ\text{C}$) (Ref. 26) and somewhat further from the $\sim 800\text{ cm}^{-1}$ librational band in polycrystalline ice (at 266 K).²⁷ A similarly broad band at 698 cm^{-1} is observed in the room temperature resonance Raman spectrum of the hydrated electrons in a liquid water jet.⁶

Some insights on the hydrogen bonding network can be extracted from the spectra measured in the water librational region ($550\text{--}1000\text{ cm}^{-1}$). In the $n=15$ spectrum, band A extends from 570 to 800 cm^{-1} , with an absorption maximum at $\sim 710\text{ cm}^{-1}$. The width of this band increases considerably with cluster size mainly toward shorter wavelengths, indicating the formation of stronger hydrogen bonds with cluster size, while its maximum gradually moves to longer wavelengths, suggesting a weakening of the hydrogen bonding network on average, and is found at 683 cm^{-1} in $n=50$, close to the value found for liquid water. Overall, band A shows the smallest dependence on cluster size of the three bands.

Band C, found at 1618 cm^{-1} in the $n=15$ spectrum, is rather broad, extending from ~ 1590 to 1700 cm^{-1} , and has a pronounced asymmetric shape. From a comparison to the calculated and experimental spectra of smaller water clusters, e.g., $(\text{H}_2\text{O})_6^-$ and $(\text{H}_2\text{O})_8^-$,^{17,28} the asymmetric shape can be traced back to be the result of multiple bending modes of water molecules in slightly different hydrogen-bonded environments. Band C broadens with increasing cluster size. Interestingly, its peak position remains at $\sim 1610\text{ cm}^{-1}$ until $n=25$, close to the band maximum found in the Raman spectrum of solvated electrons (1609 cm^{-1}).⁶ For larger clusters band C monotonically shifts to higher frequencies, up to 1637 cm^{-1} in $n=50$, close to the value of the water bending band in ice (1630 cm^{-1}) (Ref. 27) and in liquid water (1640 cm^{-1}),⁶ suggesting that the band position has converged to the value of bulk water.

The spectral region between 1450 and 1600 cm^{-1} is particularly interesting, as it reflects the bending motion of water molecules interacting more strongly with the excess electron. Band B monotonically redshifts from 1518 cm^{-1} in $n=15$ to 1497 cm^{-1} in $n=20$. Between $n=25$ and 35 , band B broadens and its maximum exhibits a small but distinct blue-shift of 15 cm^{-1} , and a new feature emerges between the maxima of bands B and C. Above $n=35$, band B has largely evolved into a broad absorption in the $1475\text{--}1600\text{ cm}^{-1}$ region. The minimum observed in the vibrational frequency of band B between $n=20$ and $n=25$ indicates that charge transfer of electron density into the σ^* orbital of the unique, AA water molecule is largest at this point. The subsequent blue-shifting and broadening suggest that the excess electron is beginning to interact directly with multiple water molecules.

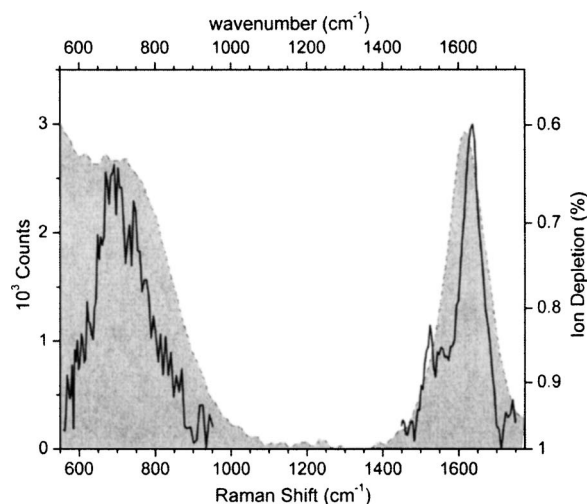


FIG. 2. Comparison of the resonance-enhanced Raman spectrum of aqueous solvated electrons (gray broken line, gray shaded, from Ref. 6) to the IRMPD spectra of $(\text{H}_2\text{O})_{45}^-$ (black line) in the region from 550 to 1775 cm^{-1} .

Interestingly, some intensity remains at 1500 cm^{-1} even at $n=50$, indicating that the original AA motif observed in the smaller clusters contributes also at larger cluster sizes, but the electron is now also interacting strongly with other water molecules, similar to the results seen for smaller type II cluster anions.¹⁷

By $n=50$, the bend and librational peaks have essentially converged to those of liquid water, with the main signature of the electron being the broad component of the bend band. However, at an estimated ion internal temperature of close to 20 K , the hydrated electron clusters are not liquid and the question arises as to why the $n=50$ spectrum in the region of the librational modes resembles that of liquid water more than that of ice. We attribute this observation to the finite size of the cluster examined here. In neutral water clusters, the onset of crystallinity occurs somewhere in the size range from 200 to 1000 water molecules,²⁹ i.e., at much larger cluster sizes than probed here. Smaller water clusters correspond to quasispherical nanoparticles with a crystal interior and a disordered “reconstructed” surface,³⁰ while even smaller clusters contain only “surface” water molecules. The reconstruction of the cluster surface may lead to a weakening of the hydrogen bonding network and thus a redshift of the librational band in the present IRMPD spectra compared to the IR spectrum of bulk ice.

In Fig. 2, we plot the present data for $n=45$ together with the resonance Raman spectrum of hydrated electrons in aqueous solution.⁶ Care has to be taken in comparing the two types of spectra. The resonance-enhanced signal in the Raman spectra is due mainly to vibrational modes that couple strongly to the electronic excitation of the confined electron, while the IRMPD spectra behave more like IR absorption spectra in that they reflect all IR-active modes of the cluster. However, the two types of spectra agree surprisingly well. The maximum of the water bending band in the resonance Raman spectrum lies between the maxima of bands B and C, i.e., where the broad feature lies that we attribute to the interaction of the electron with multiple water molecules. In-

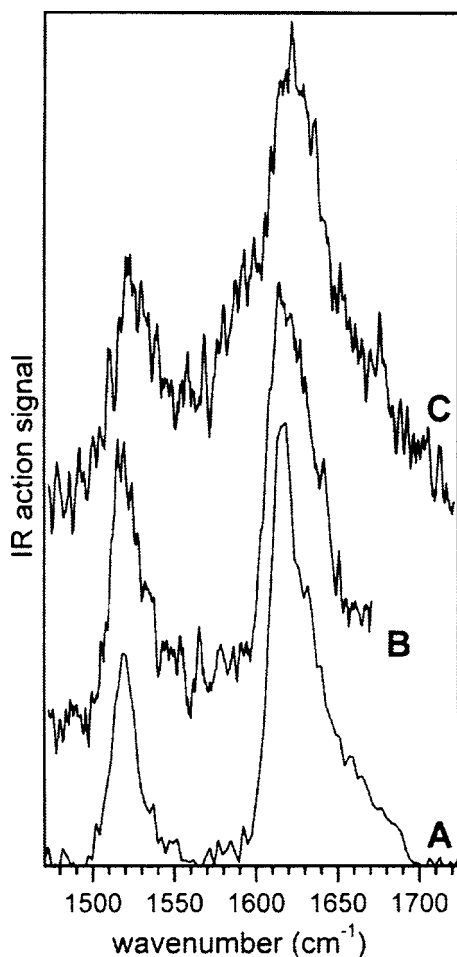


FIG. 3. Comparison of the IRMPD spectrum of bare $(\text{H}_2\text{O})_{15}^-$, labeled A (present study), to the predissociation spectra of “hot” bare $(\text{H}_2\text{O})_{15}^-$ (B) and of $(\text{H}_2\text{O})_{15}^- \cdot \text{Ar}$ (C) from Ref. 16.

terestingly, this Raman band extends down to 1400 cm^{-1} and shows substantial signal in the $1400\text{--}1550 \text{ cm}^{-1}$ region. This region is specific to the AA-binding motif in the IRMPD spectra of the clusters, leading support to the idea that this motif may be important also in the bulk.

In order to gain insight into the nature of the isomer(s) probed in the present experiment, we compare our IRMPD spectrum of $n=15$ (spectrum A in Fig. 3) to the predissociation spectra of Roscioli *et al.*¹⁶ of bare $(\text{H}_2\text{O})_{15}^-$ and $(\text{H}_2\text{O})_{15}^- \cdot \text{Ar}$, measured in a linear action mode using a tabletop OPO/OPA laser system. In that study, the isomer distributions in the ion ensembles were determined with photoelectron spectroscopy, showing that the bare cluster was prepared exclusively as isomer I, while I and II both contributed to the Ar-tagged species. Good agreement is found between the two IR spectra of bare $(\text{H}_2\text{O})_{15}^-$, clearly indicating that the same isomeric class, i.e., isomer I, is probed in both experiments. Interestingly, the Ar-tagged spectrum (C) is blueshifted, broader, and displays an additional shoulder at 1590 cm^{-1} , consistent with expectations for the spectra of a mixed ensemble of isomers I and II. In particular, the shoulder likely results from a kinetically trapped higher-energy structure (II), which is clearly not present in the IRMPD spectrum of the collisionally cooled ions in the present experiment.

Thus, the following picture of electron solvation in finite water clusters emerges from our study. (i) Electron binding in the clusters up to $n=20\text{--}25$ is dominated by the AA-binding motif, i.e., binding to predominantly a single water molecule, which is dipole oriented and points its two hydrogen atoms into the electron cloud. (ii) Starting between $n=20$ and $n=25$, other water molecules directly interact with the additional electron. As the cluster grows, the AA motif remains, but part of the electron density is now delocalized over multiple water molecules. We note that at $n \sim 25$, there is a change of slope in both the VDEs (an observation that was not explicitly reported in previous work⁹) and excited state lifetimes¹¹ of the isomer I clusters, providing further support for evolution of the electron binding motif in this size range. (iii) No abrupt changes in the IRMPD spectra are observed in the range from $n=15$ to $n=50$, supporting the notion of a gradual transition in the way the hydrogen-bonded water network binds the excess electron. Summarizing, vibrational spectroscopy yields important insight into the binding motif of the hydrated electron in finite clusters. However, it may be unable to answer convincingly the question of internal versus surface solvation, even when IR spectra of larger water cluster anions become available.

The authors gratefully acknowledge the support of the Stichting voor Fundamenteel Onderzoek der Materie (FOM) in providing the required beam time on FELIX and highly appreciate the skillful assistance of the FELIX staff. K.R.A. and G.S. thank the Deutsche Forschungsgemeinschaft for support as part of the GK788 and SFB546. D.M.N. thanks the Air Force Office of Scientific Research for support under Grant No. F49620-03-1-0085. M.A.J. thanks the Department of Energy for support under Grant No. DE-FG02-06ER15800. E.G. thanks the National Science and Engineering Research Council of Canada for a postgraduate scholarship. K.R.A. thanks G. Meijer for his continuous support and valuable discussions.

¹L. Kevan, *Radiat. Phys. Chem.* **17**, 413 (1981).

²S. A. Dikanov and Y. D. Tsvetkov, *Electron Spin Echo Envelope Modulation (ESEEM) Spectroscopy* (CRC, Boca Raton, FL, 1992).

³B. J. Schwartz and P. J. Rossky, *J. Chem. Phys.* **101**, 6917 (1994).

⁴J. C. Alfano, P. K. Walhout, Y. Kimura, and P. F. Barbara, *J. Chem. Phys.* **98**, 5996 (1993).

⁵M. Mizuno and T. Tahara, *J. Phys. Chem. A* **105**, 8823 (2001); M. J. Tauber and R. A. Mathies, *ibid.* **105**, 10952 (2001).

⁶M. J. Tauber and R. A. Mathies, *J. Am. Chem. Soc.* **125**, 1394 (2003).

⁷H. Haberland, H. G. Schindler, and D. R. Worsnop, *Ber. Bunsenges. Phys. Chem.* **88**, 270 (1984).

⁸J. V. Coe, G. H. Lee, J. G. Eaton, S. T. Arnold, H. W. Sarkas, K. H. Bowen, C. Ludewigt, H. Haberland, and D. R. Worsnop, *J. Chem. Phys.* **92**, 3980 (1990); J. V. Coe, S. T. Arnold, J. G. Eaton, G. H. Lee, and K. H. Bowen, *ibid.* **125**, 014315 (2006); J. Kim, I. Becker, O. Cheshnovsky, and M. A. Johnson, *Chem. Phys. Lett.* **297**, 90 (1998); A. Kamrath, J. R. R. Verlet, G. B. Griffin, and D. M. Neumark, *J. Chem. Phys.* **125**, 171102 (2006).

⁹J. R. R. Verlet, A. E. Bragg, A. Kamrath, O. Cheshnovsky, and D. M. Neumark, *Science* **307**, 93 (2005).

¹⁰A. E. Bragg, J. R. R. Verlet, A. Kamrath, O. Cheshnovsky, and D. M. Neumark, *Science* **306**, 669 (2004); D. H. Paik, I.-R. Lee, D.-S. Yang, J. S. Baskin, and A. H. Zewail, *ibid.* **306**, 672 (2004).

¹¹A. E. Bragg, J. R. R. Verlet, A. Kamrath, O. Cheshnovsky, and D. M. Neumark, *J. Am. Chem. Soc.* **127**, 15283 (2005).

¹²R. N. Barnett, U. Landman, C. L. Cleveland, and J. Jortner, *J. Chem. Phys.* **88**, 4429 (1988).

- ¹³L. Turi, W.-S. Sheu, and P. J. Rossky, *Science* **309**, 914 (2005).
- ¹⁴P. Ayotte and M. A. Johnson, *J. Chem. Phys.* **106**, 811 (1997).
- ¹⁵P. Ayotte, C. G. Bailey, J. Kim, and M. A. Johnson, *J. Chem. Phys.* **108**, 444 (1998); N. I. Hammer, J.-W. Shin, J. M. Headrick, E. G. Diken, J. R. Roscioli, G. H. Weddle, and M. A. Johnson, *Science* **306**, 675 (2004); N. I. Hammer, J. R. Roscioli, J. C. Bopp, J. M. Headrick, and M. A. Johnson, *J. Chem. Phys.* **123**, 244311 (2005).
- ¹⁶J. R. Roscioli, N. I. Hammer, and M. A. Johnson, *J. Phys. Chem. A* **110**, 7517 (2006).
- ¹⁷J. R. Roscioli and M. A. Johnson, *J. Chem. Phys.* **126**, 0243071 (2007).
- ¹⁸J. M. Herbert and M. Head-Gordon, *J. Am. Chem. Soc.* **128**, 13932 (2006).
- ¹⁹T. Sommerfeld and K. D. Jordan, *J. Am. Chem. Soc.* **128**, 5828 (2006).
- ²⁰K. R. Asmis, M. Brümmer, C. Kaposta, G. Santambrogio, G. von Helden, G. Meijer, K. Rademann, and L. Wöste, *Phys. Chem. Chem. Phys.* **4**, 1101 (2002).
- ²¹D. Oepts, A. F. G. van der Meer, and P. W. van Amersfoort, *Infrared Phys. Technol.* **36**, 297 (1995).
- ²²U. Even, J. Jortner, D. Noy, N. Lavie, and C. Cossart-Magos, *J. Chem. Phys.* **112**, 8068 (2000).
- ²³M. A. Johnson and W. C. Lineberger, in *Techniques of Chemistry*, edited by J. M. Farrar and W. H. Saunders, Jr. (Wiley, New York, 1988), Vol. 20, p. 591.
- ²⁴G. von Helden, I. Holleman, G. M. H. Knippels, A. F. G. van der Meer, and G. Meijer, *Phys. Rev. Lett.* **79**, 5234 (1997); J. Oomens, A. G. G. M. Tielens, B. G. Sartakov, G. von Helden, and G. Meijer, *Astrophys. J.* **591**, 968 (2003).
- ²⁵M. K. Beyer, B. S. Fox, B. M. Reinhard, and V. E. Bondybey, *J. Chem. Phys.* **115**, 9288 (2001).
- ²⁶H. R. Zelsmann, *J. Mol. Struct.* **350**, 95 (1995).
- ²⁷S. G. Warren, *Appl. Opt.* **23**, 1206 (1984).
- ²⁸N. I. Hammer, J. R. Roscioli, and M. A. Johnson, *J. Phys. Chem. A* **109**, 7896 (2005).
- ²⁹G. Torchet, P. Schwartz, J. Farges, M. F. Deferaudy, and B. Raoult, *J. Chem. Phys.* **79**, 6196 (1983).
- ³⁰V. Buch, S. Bauerecker, J. P. Devlin, U. Buck, and J. K. Kazimirski, *Int. Rev. Phys. Chem.* **23**, 375 (2004).